DETC2006-99048

AN INTRODUCTION TO THE ANALYSIS OF LINKAGE-DRIVEN COMPLIANT UNDERACTUATED FINGERS

Lionel Birglen
Department of Mechanical Engineering,
École Polytechnique of Montréal,
Montréal, Qc, H3T 1J4, Canada,
lionel.birglen@polymtl.ca

ABSTRACT

This paper presents an analysis of a two-phalanx linkage-driven underactuated finger with substantial compliance in all the joints of the system. The primary goal of the paper is to illustrate with an example, the theoretical issues faced in designing compliant underactuated fingers. To this aim, a two-phalanx linkage-driven underactuated finger is analyzed throughout the paper to clarify the concepts presented. First, a method to compute the contact forces generated by compliant underactuated fingers is presented and discussed. Finally, the self-mobility of the finger is discussed and a method to predict if this mobility will converge to a stable grasp or not is presented. The paper presents an exemplified theoretical analysis whose layout provides very useful insights for the design of compliant underactuated fingers and emphasizes the challenges to be met in order to design successful prototypes.

Introduction

The lack of success of complex robotic hands in the past has mainly been attributed to the cost and complexity of these systems with numerous actuators and sensors requiring a heavy control architecture. In order to overcome these limitations, a particular emphasis has been placed on the reduction of the number of degrees of freedom, thereby decreasing the number of actuators. In the past few years, many prototypes have been proposed taking advantage of *underactuation* [Hirose and Umetani(1978), Laliberté and Gosselin(1998), Herder and Visser(2000), Dubey and Crowder(2002), Carrozza *et al.*(2003), Krut(2005)]. The latter involves a smaller number of actuators without decreasing the number of degrees of freedom and can be implemented through the use of passive elements like springs and requires a dedicated transmission technique. The main advantage of this method is a mechanical adaptation of the finger to the shape of the object to be grasped. This adaptation is realized without a dedicated control law, e.g. a constant actuator torque is usually sufficient to achieve this property. Shape-adaptation to the grasped object is often of uttermost importance to ensure a secure grasp. If manipulation of the object is desired, the latter can be realized with the arm to which the gripper is fastened. Therefore, manipulation is often not a very important characteristic for robotic hands and fingers, at least for devices aiming at industrial applications. Nevertheless, most of the robotic hands developed by the research community over the last two decades have tried to imitate the human hand in terms of manipulation capability. Underactuation in robotic hands aims to be an intermediate technological solution between simple mechanical grippers and complex robotic hands. From the former it aims at keeping a very limited number of actuators while realizing difficult grasping tasks with performances similar to the latter. Grasping in unstructured environments is a major challenge for robotic hands with applications ranging from space/subsea robotics to computer assisted surgery, and underactuation is a promising technology to achieve this task efficiently.

Underactuation in Grasping and Compliant Mechanisms

Underactuation in robotic fingers is different from the concept of underactuation usually presented in robotic systems and both notions should not be confused. Underactuated fingers generally use elastic elements in the design of their "unactuated" joints. Thus, one should rather think of these joints as *uncontrollable* or *passively driven* instead of unactuated. In underactuated fingers, the actuation wrench T_a is applied to the input of the finger and is transmitted to the phalanges through suitable mechanical elements, e.g. four-bar linkages [Gosselin and Laliberté(1996)], pulleys and tendons [Hirose and Umetani(1978)], gears [Birglen and Gosselin(2004)], etc. Passive elements are used to kinematically constrain the finger and ensure the shape-adaptation of the finger to the object grasped. The type of underactuated two-phalanx finger considered in this paper and its closing sequence are illustrated in Fig. 1. The actuation torque T_a is applied to the first link which transmits the effort to both phalanges. Notice the mechanical limit that allows a pre-loading of the spring to prevent any undesirable motion of the second phalanx due to its own weight and/or inertial effects, and also to prevent hyperextension of the finger. Springs are useful for keeping the finger from incoherent motion, but when the grasp sequence is complete, they still oppose the actuator force. Therefore, this compliance in the finger itself is usually kept small and neglected. However, this is not always possible, especially in the case of a finger built using structural compliant joints. In that case, compliance in all the joints of the finger, including in the transmission mechanism, should be taken into account. This additional compliance in the transmission mechanism is the main difference between usual underactuated fingers and the analysis proposed in this paper.

Compliant mechanisms are defined as mechanical architectures in which motion and force are transmitted among various members of the system through relative flexibility. They have recently attracted a lot of attention from researchers around the world. Indeed, these mechanisms can eliminate usual mechanical drawbacks such as wear, clearance or backlash and are also very interesting for small-scale mechanisms such as micro electro-mechanical systems. Yet, if the analysis of general compliant mechanisms is fairly well documented [Howell(2001), Lobontiu(2002)], the analysis of compliant underactuated fingers from a theoretical point of view is almost non-existent despite a handful of very interesting prototypes [Massa and Gosselin(2003), Carrozza *et al.*(2005), Lotti *et al.*(2005), Boudreault and Gosselin(2005)]. This paper aims at proposing a method to analyze compliant underactuated fingers. This method and its results are presented using the example of a linkage-driven two-phalanx underactuated finger but the framework adopted in this paper remains valid with any architecture providing that the expressions of the kinetostatic analysis are modified accordingly. It should be emphasized that the issues concerning the compliant material itself, such as stresses or failure, are not directly addressed in this paper, despite their importance. Rather, attention is focused on the particular challenges that should be met when designing compliant underactuated fingers. Readers interested in a more general analysis of compliant mechanisms, flexures, and/or material issues are referred to the available textbooks [Smith(2000), Howell(2001), Lobontiu(2002)].

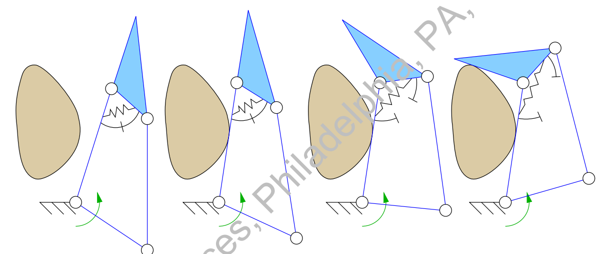

Figure 1. Closing sequence of a two-phalanx finger with linkage transmission.

Kinetostatic Analysis

The particular design of compliant two-phalanx underactuated finger using a four-bar linkage transmission mechanism used in this paper is detailed in Fig. 2. The equivalent design without compliance in the transmission linkage is well documented [Birglen and Gosselin(2004), Birglen and Gosselin(2006)] with several prototypes [Gosselin and Laliberté(1996), Laliberté and Gosselin(2003), Luo *et al.*(2004)]. The actuation torque T_a is applied to the link a which transmits the effort to the phalanges through link b.

A simple kinetostatic model for the finger with compliant joints can be obtained by adding springs to every joints of the finger. However, the double joint initially located in point O_1 might be difficult to obtain with compliant mechanisms. Hence, these two joints are separated in this analysis. However, it is assumed that the distance between the resulting separated joints is kept small as it allows to consider the transmission mechanism as a four-bar linkage instead of a five-bar linkage. This hypothesis considerably simplify the analysis. Thereupon, two choices are possible for the attachment of the actuation link a, illustrated in Fig. 3. Either this link is attached to the ground or to the proximal phalanx. Both cases are considered in the analysis.

The complete kinetostatic analysis of underactuated fingers with non-compliant transmissions has been presented in [Birglen and Gosselin(2004)] and yielded surprising results. For instance,

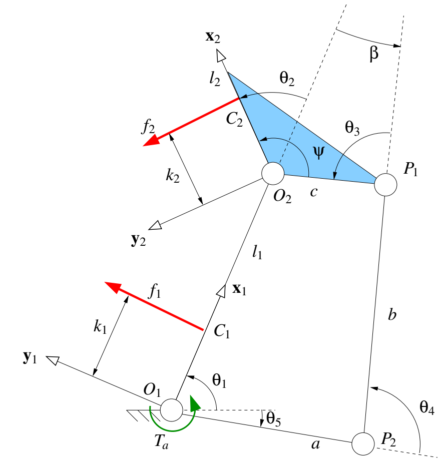

Figure 2. Two-phalanx underactuated finger model.

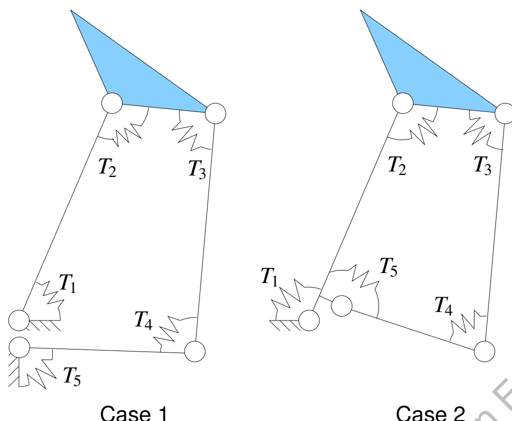

Figure 3. The two possible kinetostatic models of the finger.

once the contact forces developed by underactuated fingers have been established it has been shown that there exist configurations where an underactuated finger cannot apply forces to an object. Indeed, in certain grasp-states, some contact forces may be negative. A grasp state is defined as the set of the geometric configuration of the finger and the contact locations on the phalanges necessary to characterize the behaviour of the finger (sign of the contact forces, grasp stability, etc.) If a situation where a contact force is negative, the finger undergoes a motion, referred to as self-posture changeability [Kaneko and Hayashi(1993)], that either converges to a stable grasp or lead to the ejection of the object from the finger [Birglen and Gosselin(2006)]. It should be pointed out that with two-phalanx underactuated fingers, the occurrence of a negative proximal contact force cannot be eliminated regardless of the transmission mechanism used [Birglen and Gosselin(2006)]. Since underactuated fingers using compliant transmissions take advantage of the same technique than the fingers described in previous works, it is natural to expect the same phenomenon to occur. Therefore, the analysis of the contact forces is of uttermost importance, if only as a basis to an optimization procedure, in order to reduce the occurrence of this phenomenon. The contact forces are established for the two-phalanx models presented in Fig. 3 with a kinetostatic analysis. Equating the input and the output virtual powers of the finger, one obtains

$$\mathbf{t}^T \omega_a = \mathbf{f}^T \mathbf{v} \tag{1}$$

where $\mathbf{t}$ is the input torque vector exerted by the actuator and the springs, ω_a is the corresponding velocity vector, $\mathbf{f}$ is the vector of contact forces, and $\mathbf{v}$ is the vector of the projected velocities of the contact points. i.e.:

$$\mathbf{t} = \begin{bmatrix} T_a \\ T_1 = -K_1\Delta\theta_1 \\ T_2 = -K_2\Delta\theta_2 \\ \cdots \\ T_5 = -K_5\Delta\theta_5 \end{bmatrix}, \quad \omega_a = \begin{bmatrix} \dot{\theta}_a \\ \dot{\theta}_1 \\ \dot{\theta}_2 \\ \cdots \\ \dot{\theta}_5 \end{bmatrix}. \tag{2}$$

and

$$\mathbf{f} = \begin{bmatrix} f_1 \\ f_2 \end{bmatrix}, \ \mathbf{v} = \begin{bmatrix} \mathbf{v}_{C_1}^T \mathbf{y}_1 \\ \mathbf{v}_{C_2}^T \mathbf{y}_2 \end{bmatrix}, \tag{3}$$

where K_i is the stiffness of the torsional spring associated with θ_i. Furthermore, $\mathbf{v}$ can be expressed as the product of a Jacobian matrix $\mathbf{J}$ and the derivatives of the phalanx joint coordinates, i.e. $\mathbf{v} = \mathbf{J}\dot{\theta}$ with $\theta = [\theta_1 \ \theta_2\ ]^T$. Similarly, one can also establish the matrix $\mathbf{T}_c$ which relates the vector ω_a to the derivatives of the phalanx joint coordinates, i.e. $\omega_a = \mathbf{T}_c\dot{\theta}$. This matrix contains elements which are function of the transmission mechanism used in the finger. The analytical expressions of both matrices in case of a non-compliant transmission has been established in [Birglen and Gosselin(2004)]. It should be noted that the expression of matrix $\mathbf{J}$ does not change in the case of a compliant transmission since it is only function of the finger kinematic parameters and is therefore independent of the transmission mechanism. Conversely, the transmission matrix $\mathbf{T}_c$ has to be modified (hence the subscript c to indicate compliance). Also, it should be emphasized that the second form of the transmission matrix presented in [Birglen(2004)] has been used since it does not require the inversion of the latter to compute the contact forces (the matrix is not square in this case). Eq. (1) then becomes

$$\mathbf{f} = \mathbf{J}^{-T}\mathbf{T}_c^T\mathbf{t}, \tag{4}$$

The latter equation can be separated in two in order to emphasize the effect of the compliance in the transmission, namely

$$\mathbf{f} = \mathbf{A}\mathbf{t}_f + \mathbf{B}\mathbf{t}_t, \tag{5}$$

where $\mathbf{t}_f = [T_a\ T_1\ T_2]^T$ is the vector of the actuation torque and the compliance in the finger structure while $\mathbf{t}_t = [T_3\ T_4\ T_5]^T$ characterizes the compliance in the transmission linkage. Combining eqs. (4) and (5), one obtains

$$\mathbf{A} = \mathbf{J}^{-T}\mathbf{T}^T \quad \text{and} \quad \mathbf{B} = \mathbf{J}^{-T}\mathbf{T}_\star^T \tag{6}$$

where $\mathbf{T}$ is the transmission matrix of the finger without compliance in the transmission while $\mathbf{T}_\star$ accounts for the latter. Both matrices are defined with

$$\mathbf{T}_c = \begin{bmatrix} \mathbf{T} \\ \mathbf{T}_\star \end{bmatrix} \tag{7}$$

Using the basic kinematic equations of four-bar linkages [McCarthy(2000)], one obtains

$$\mathbf{T}_c^T = \begin{bmatrix} 1 & 1 & 0 & 0 & 0 & \delta \\ \frac{h}{h+l_1} & 0 & 1 & \frac{h_c+c}{h_c} & -\frac{(h_a+a)h}{h_a(h+l_1)} & \frac{h}{h+l1} \end{bmatrix} \tag{8}$$

where h is the signed distance between point O_2 and the geometric intersection of lines (O_1O_2) and (P_1P_2). Similarly h_a and h_c are the signed distances between the intersection of lines (O_1P_2) and (O_2P_1), and points P_2 and P_1 respectively. Therefore, using the expression of the Jacobian matrix $\mathbf{J}$ found in the literature, one finally obtains

$$\mathbf{A} = \begin{bmatrix} \frac{l_1(k_2-h\cos\theta_2)}{k_1k_2(h+l_1)} & \frac{1}{k_1} & -\frac{k_2+l_1\cos\theta_2}{k_1k_2} \\ \frac{h}{k_2(h+l_1)} & 0 & \frac{1}{k_2} \end{bmatrix} \tag{9}$$

and

$$\mathbf{B}^T = \begin{bmatrix} -\frac{(k_2+l_1\cos\theta_2)(h_c+c)}{k_1k_2h_c} & \frac{h_c+c}{k_2h_c} \\ \frac{(k_2+l_1\cos\theta_2)(h_a+a)h}{k_1k_2(h+l_1)h_a} & -\frac{(h_a+a)h}{k_2(h+l_1)h_a} \\ \frac{\delta}{k_1} - \frac{h(k_2+l_1\cos\theta_2)}{k_1k_2(h+l_1)} & \frac{h}{k_2(h+l_1)} \end{bmatrix} \tag{10}$$

with

$$\begin{cases} \delta = 1 \text{ in case 1} \\ \delta = 0 \text{ in case 2} \end{cases} \tag{11}$$

This simple expression of the difference between the two kinetostatic models arises from the velocity relationship between $\dot{\theta}_5$ and $\dot{\theta}_2$, namely

$$\begin{cases} \dot{\theta}_5 = \dot{\theta}_1 + \frac{h}{h+l_1}\dot{\theta}_2 \text{ in case 1} \\ \dot{\theta}_5 = \frac{h}{h+l_1}\dot{\theta}_2 \qquad \text{in case 2} \end{cases} \tag{12}$$

Therefore, one can easily compute the contact forces using eq. (5) as functions of the actuation vector and for any grasp-state of the finger, namely $(\theta_1, \theta_2, k_1, k_2)$. In the case of a compliant transmission, it is a reasonable hypothesis that the compliances in the joints are not negligible. Hence, the next required step is to obtain the expressions of the spring torques in all the joints of the finger. Basically two possible types of compliant joints can be used: living or notch hinges, as illustrated in Fig. 4. Living hinges are inserts of low stiffness elastic material in replacement of the joints. The main advantage of this type of joint is that the comparatively low stiffness of the inserted material is sometimes neglected. However, if this is not accurate, the rotational stiffness of this type of joint can be approximated [Howell and Midha(1994)] from cantilever beam theory to

$$K_i = \frac{EI}{L} \tag{13}$$

where E is the elastic modulus of the material inserted, I is the cross-sectional moment of inertia of the insert and L is the length of the joint.

Notch hinges are geometric patterns directly machined in the structure of the system. If notch type circular hinges are selected, the rotational stiffness of the latter can be estimated to [Smith(2000)]

$$K_i = \frac{2Ebt^{5/2}}{9\pi\sqrt{R}} \tag{14}$$

where E is again the elastic modulus of the material constituting the finger, b and t are respectively the off-the-plane axis and transverse thicknesses of the joint, while R is the radius of the joint (cf. Fig. 4). The main advantage of notch type hinges is that they do not require any assembly and can be machined directly from the structure of the finger. Notice that in this case, a circular geometry hinge has been arbitrarily chosen as an example but many other exist [Lobontiu(2002)]: elliptic, hyperbolic, parabolic, corner-filleted, rectangular, etc.

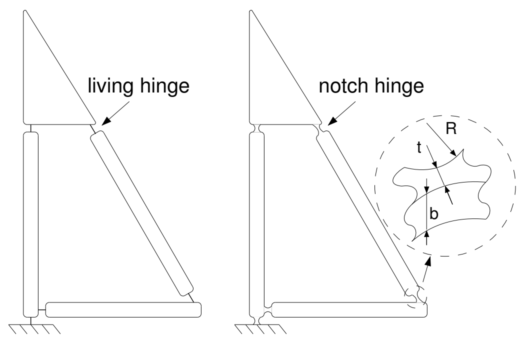

Figure 4. Design of the compliant joints.

Once all the parameters defining the finger are chosen, one can compute the contact forces as functions of the grasp-state. An example of the evolution of the contact forces is presented in Fig. 5 where the parameters of Table 1 have been chosen for the geometry of the finger. Furthermore, the attachment of the actuation link corresponds to case 2. For the joints, five identical notch hinges have been selected with a geometry defined by $(b,t,R) = (15, 0.75, 5)$ millimeters. The joints (and the finger) of this example are made from polypropylene, a thermoplastic polymer commonly used in compliant mechanisms with a Young's Modulus $E = 1.39$ GPa. The configuration where $\theta_1 = \theta_2 = 0$ has been chosen to correspond to the resting configuration of the finger, i.e. with no deflection of any joints (hence all spring torques are zero), and the contacts are assumed to be located at mid-phalanx, i.e. $k_1 = l_1/2$ and $k_2 = l_2/2$. These assumptions have been made to illustrate the points discussed in the paper, but the presented method can be used with any other grasp-state, geometry, etc.

Table 1. Geometric parameters of the finger (in mm)

l_1	l_2	ψ	a	b	c
60	40	90°	50	60	20

An important and typical phenomenon that can be observed in this example is the vanishing of the contact force f_2. The fact that f_1 can become negative was expected, but not f_2. With a

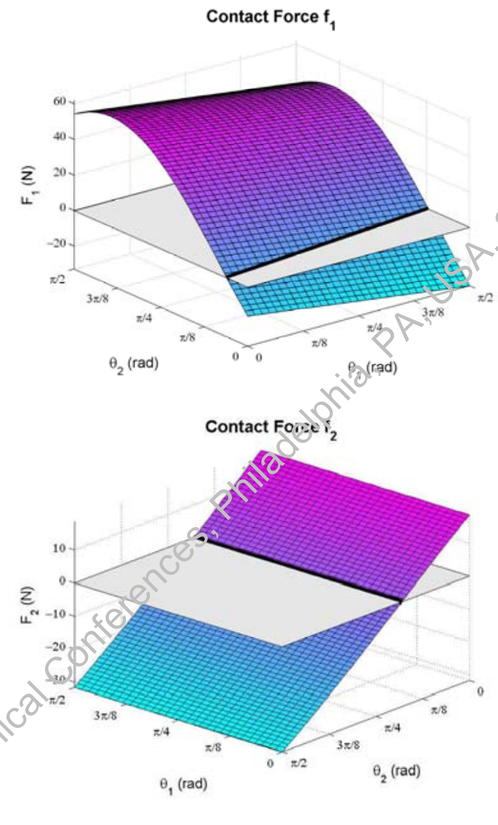

Figure 5. Evolution of the contact forces for a unitary actuation torque ($T_a = 1$ N.m).

non-compliant transmission, f_2 only becomes negative in rare hyperflexion/hyperextension configurations that are usually outside the workspace of the finger [Birglen and Gosselin(2006)]. With compliant transmissions this transition to a negative contact force may happen in the usual workspace of the finger if the spring torques generated by the compliance of the joints overcome the actuation torque T_a. This has to be prevented by using eq. (5) and ensure that $f_2 = 0$ has no solution in the desired workspace. The analytical expressions are complicated due to the presence of all the internal angles of the transmission linkage but can solved numerically nonetheless. In the case of the example depicted in Fig. 5, one obtains the condition $T_a > 3.535$ N.m for the actuation torque.

By carefully studying the results obtained with eq. (5), one can also decide which one of case 1 or 2 is the more suitable choice. The main difference between the two cases, arising from the kinetostatic analysis, is that the compliance torque T_5 in case 1 is basically opposed to the actuation torque while the situation is more complex in case 2. Indeed, in the latter case, the opposition to the actuation torque is also present but modulated by the reaction of the spring modeling the compliance T_5. This reaction is applied to the proximal phalanx and creates a torque at the base joint O_1 which is "increasing" the actuation torque. This effect yields that the value of the contact force f_1 is typically higher in case 2 than in case 1. At first, it might therefore be preferable to use the case 2 solution since it decreases the relative magnitude of the opposing torques due to the compliance in the transmission linkage. However, one has to be careful since the increase of f_1 might be detrimental to the quality of the grasp with respect to force-isotropy [Birglen and Gosselin(2004)]. Indeed, the contact forces generated by an underactuated finger usually significantly decrease for the distal phalanges, i.e. the proximal phalanges are usually much stronger than the distal phalanges. This might be an issue if grasping delicate objects is considered, because the actuation torque required to overcome the compliance in the joints to close the distal phalanges can generate a contact force on the proximal phalanges exceeding the maximal admissible force. Additionally, because of the structure of the finger in case 2, the angle θ_5 has a limited range of value over the workspace of the finger since it does not change with θ_1. Conversely, in case 1, the values of θ_5 required to cover the workspace are typically much larger. Hence, for the same stiffness K_5, the torque T_5 has usually larger values in case 1 and is therefore more penalizing. This is especially of concern if the value of f_2 is low.

Therefore, the selection of case 1 or 2 depends on the primary criterion chosen by the designer:

- if force-isotropy is desired, case 1 should be selected;
- if the opposing torques due to the joints are large and close to the actuation torque, case 2 should be selected.

To summarize, the analysis of the contact forces is of uttermost importance when designing underactuated fingers since once the finger is built, only one control variable is available to the user, namely the actuation torque value. The relative magnitude of the contact forces cannot be controlled with underactuated fingers and therefore, has to be carefully analyzed during the design stage. This statement is even more accurate in the case of a compliant transmission linkage mechanisms since this compliance might seriously interfere with the actuation torque and generate new phenomena such as the vanishing of the distal contact force.

Grasp Stability

In order to determine the configurations where a two-phalanx compliant underactuated finger can apply forces to the object grasped, a quasi-static model was developed in the previous section. It is assumed in this section that the actuation torque is large enough to prevent f_2 from becoming negative, e.g. $T_a = 4$ N.m with the example depicted in Fig. 5. However, even in this case, f_1 can become negative. If the finger has finished its closing sequence on the object and the grasp-state $(\theta_1, \theta_2, k_1, k_2)$ corresponds to a negative proximal force f_1, this contact will be lost. Thereupon, the distal phalanx will slide on the object until either a stable grasp, defined as a situation where the finger is in static equilibrium, is achieved or ejection occurs ($k_2 > l_2$, illustrated in Fig. 6).

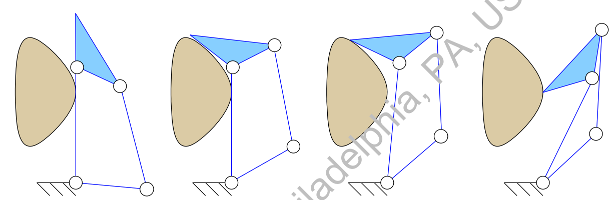

Figure 6. Example of an ejection sequence.

It is important to note that with underactuated fingers, a stable grasp is a contact situation with no negative contact forces, or more precisely, a grasp is stable if and only if the finger is in static equilibrium. Stable grasps, as they are referred to should not be confused with form- or force-closure as usually defined in the literature. The concept of grasp stability with underactuated fingers is fundamentally different than with fully actuated robotic hands. Indeed, with the latter, a static equilibrium can always be achieved. Conversely, equilibrium cannot be always ensured using underactuated fingers. Also, it should be noted that the contacts are assumed to be fixed in space in this analysis.

The sliding process of the finger can be characterized by the evolution of a reduced grasp-state, namely $(k_2, \theta_1, \theta_2)$. It should be emphasized that θ_1 has to be taken into account to evaluate the torques generated by the compliance in the joints, contrary to the usual cases of two-phalanx underactuated fingers. In the case where the compliance is neglected, one could study the behavior of the system in a grasp-state plane (k_2, θ_2). If the compliance in the joints has to be taken into account, a grasp-state space $(\theta_1, \theta_2, k_2)$ with dimension three should be used. The sliding process undergone by the finger when the proximal contact is lost defines a trajectory in the grasp-state space and the grasp-state evolves along this trajectory until a stable location is reached or ejection occurs. The condition of a stable grasp where the finger is in static equilibrium defines an equilibrium condition $f_1 = 0$ corresponding to an equilibrium surface in the grasp-state space. The contact trajectories are defined by

$$k_{2i} C_{\theta_{2i}} - k_2 C_{\theta_2} = K \qquad (15)$$

$$l_1 (1 - C_{\theta_{1i} - \theta_1}) + k_{2i} (C_{\theta_{2i}} - C_{\theta_1 - \theta_{1i} - \theta_{2i}}) = K \qquad (16)$$

with

$$K = \frac{k_2^2 - k_{2i}^2}{2l_1}, \tag{17}$$

obtained by expressing that the contact location is a point fixed in space (the law of cosines in the triangle $O_1O_2C_2$), where $(\theta_{1i}, \theta_{2i}, k_{2i})$ is an arbitrary initial contact situation on the trajectory and $C_\alpha = \cos\alpha$. Through each point of the grasp-state space passes one and only one contact trajectory. The grasp-state evolves on that contact trajectory in a direction depending on its location with respect to the equilibrium surface defined by $f_1 = 0$. The evolution of the grasp-state ends either when it attains the equilibrium surface (or a mechanical limit) or when it quits the limit of the grasp-state space (defined by $k_2 = l_2$, corresponding to ejection). The equilibrium locus of the finger is defined by $f_1 = 0$, using Eq. (5), one obtains

$$E_0 T_a + \sum_{i=1}^{5} E_i T_i = 0 \tag{18}$$

with

$$E_0 = h_c h_a l_1 (k_2 - h\cos\theta_2) \tag{19}$$
$$E_1 = k_2 h_c h_a (h + l_1) \tag{20}$$
$$E_2 = -h_c h_a (h + l_1)(k_2 + l_1\cos\theta_2) \tag{21}$$
$$E_3 = -h_a (h_c + c)(k_2 + l_1\cos\theta_2)(h + l_1) \tag{22}$$
$$E_4 = h h_c (h_a + a)(k_2 + l_1\cos\theta_2) \tag{23}$$
$$E_5 = h_c h_a (k_2 h(\delta - 1) + l_1(\delta k_2 - h\cos\theta_2)) \tag{24}$$

An example of a contact trajectory and an equilibrium surface is illustrated in Fig. 7, the parameters of the example presented in Fig. 5 were used with $T_a = 4Nm$ and $(\theta_{1i}, \theta_{2i}, k_{2i}) = (\pi/4, 0, l_2/2)$ as the initial grasp-state. Note that the contact location corresponding the equilibrium surface $k_2 = e(\theta_1,\ \theta_2)$ is larger than l_2 for certain values of $(\theta_1,\ \theta_2)$, this phenomenon has been proven to lead to ejection [Birglen and Gosselin(2006)]. The locus where the equilibrium surface contact location e leaves the limit of the grasp-state space is outlined in black in Fig. 7.

The analysis of this grasp-state space allows to predict if a grasp will converge to an equilibrium of degenerate into ejection. The contact trajectories corresponding to typical objects with arbitrary shaped in a position inside the workspace of the finger can be studied to ensure final stability. However, obtaining conditions on the design parameters that ensure that ejection cannot happen with *any* contact trajectory is still an open problem in a grasp-state space of dimension higher than two. It should be emphasized again that the self-mobility of underactuated finger is an intrinsic phenomenon taking place even if the object is fixed in space. Again, it should be emphasized that the grasp-state stability presented in this section is fundamentally different than form- or force-closure. Indeed, the latter focus on the wrench applied to the object grasped through the contact points. In our case, a preliminary step is to ensure that the finger can apply forces in the considered configuration. Furthermore, since the object is assumed here to be fixed in space this wrench is not as critical as in the case of a mobile object to be securing by the finger.

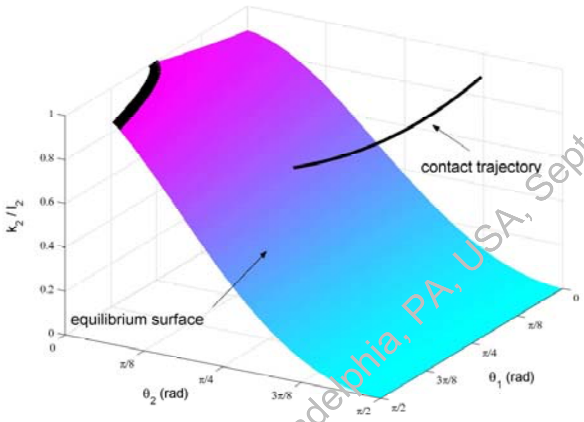

Figure 7. Equilibrium surface and contact trajectory.

Conclusion

In this paper, a step-by-step analysis of a two-phalanx linkage-driven underactuated finger with non-negligible compliance in all its joints has been presented. The method to obtain the analytical expressions of the contact forces generated by this type of finger has been emphasized. Then, in case of a negative proximal contact forces, the self-mobility of the finger and its particularity with respect to usual underactuated finger without compliance in the transmission has been discussed. The adaptation of the grasp stability theory of two-phalanx underactuated fingers to fully compliant fingers has been illustrated, and it is important to note that the method remains valid using any other mechanical transmission. What arise from the results presented in the paper is a significant increase in the complexity of the analysis: the kinetostatic expressions become rapidly cumbersome and the self-mobility has to be studied in a grasp-state space with increased dimensions. The thorough analysis of underactuated fingers with negligible compliance is already challenging and adding compliance only increases this challenge. However, it is the opinion of the author that this difficulty is worth the price. Indeed, compliant underactuated fingers can have a tremendous impact, especially in surgical robotics where compliant underactuated fingers can provide enveloping grasps, and thus, additional safety as well as a gentle distribution of the grasping forces if properly analyzed and designed. The first prototypes using this architecture have been successfully demonstrated in [Boudreault and Gosselin(2005)] but several issues remains to obtain a reliable compliant gripper with optimal performances and the first results presented in this paper, confirmed with finite element modeling (illustrated in Fig. 8) are promising. Nevertheless, as discussed in the paper many open and critical problems remain to be solved.

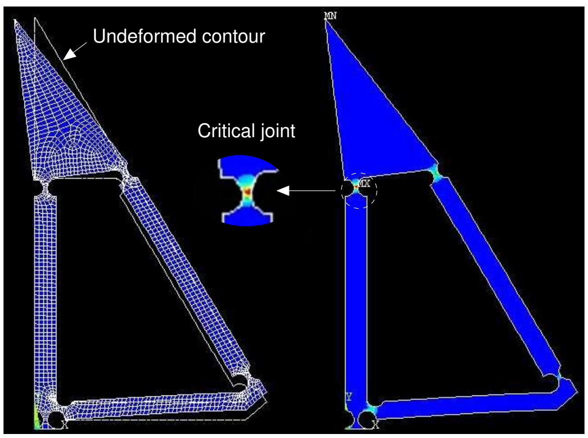

Figure 8. Numerical analysis of the deformation (left) and Von Mises stress (right).

Acknowledgments

The financial support of the Natural Sciences and Engineering Research Council of Canada (NSERC) is acknowledged.

REFERENCES

[Boudreault and Gosselin(2005)] Boudreault, É., and Gosselin, C., 2005, "Mechanically Intelligent Grippers For Telemedicine," *Poster presented at the 15th Annual Canadian Conference on Intelligent Systems*, pp. 58-72, Quebec City, Canada.

[Birglen and Gosselin(2004)] Birglen, L., and Gosselin, C., 2004, "Kinetostatic Analysis of Underactuated Fingers," *IEEE Transactions on Robotics and Automation*, 20, 2, pp. 211-221.

[Birglen(2004)] Birglen, L., 2004, "Analysis and Control of Underactuated Robotic Hands," *Ph.D. thesis, Faculté des sciences et de génie, Université Laval*, Québec, Canada.

[Birglen and Gosselin(2006)] Birglen, L., and Gosselin, C., 2006, "Grasp-State Plane Analysis of Two-Phalanx Underactuated Fingers," *Mechanism and Machine Theory (in press)*.

[Carrozza *et al.*(2003)] Carrozza, M. C., Vecchi, F., Sebastiani, F., Cappiello, G., Roccella, S., Zecca, M., Lazzarini, R., and Dario, P., 2003, "Experimental Analysis of an Innovative Prosthetic Hand with Proprioceptive Sensors," *Proceedings of the IEEE International Conference on Robotics and Automation*, pp. 2230-2235, Taipei, Taiwan

[Carrozza *et al.*(2005)] Carrozza, M. C., Cappiello, G., Stellin, G., Zaccone, F., Vecchi, F., Micera, S., and Dario, P., 2005, "A Cosmetic Prosthetic Hand with Tendon Driven Under-Actuated Mechanism and Compliant Joints: Ongoing Research and Preliminary Results," *Proceedings of the 2005 IEEE International Conference on Robotics and Automation*, pp. 2672-2677, Barcelona, Spain.

[Dubey and Crowder(2002)] Dubey, V. N., and Crowder, R. M., 2002, "A Finger Mechanism For Adaptive End Effectors," *Proceedings of 2002 ASME Design Engineering Technical Conferences*, Montreal, Canada.

[Gosselin and Laliberté(1996)] Gosselin, C., and Laliberté, T., 1996, "Underactuated mechanical finger with return actuation," *US Patent No. 5 762 390*.

[Herder and Visser(2000)] Herder, J. L., and de Visser, H., 2000, "Force Directed Design of a Voluntary Closing Hand Prosthesis," *Proceedings of the 2000 ASME Design Engineering Technical Conferences*, Baltimore, MD, USA.

[Hirose and Umetani(1978)] Hirose, S., and Umetani, Y., 1978, "The Development of Soft Gripper for the Versatile Robot Hand," *Mechanism and Machine Theory*, 13, pp. 351-358.

[Howell and Midha(1994)] Howell, L. L., and Midha, A., 1994, "A Method for the Design of Compliant Mechanisms With Small-Length Flexural Pivots," *ASME Journal of Mechanical Design*, 116, 1, pp. 280-290.

[Howell(2001)] Howell, L. L., 2001, "Compliant Mechanisms," *Wiley-Interscience*.

[Kaneko and Hayashi(1993)] Kaneko, M., and Hayashi, T., 1993, "Standing-up Characteristic of Contact Force During Self-posture Changing Motions," *Proceedings of the IEEE International Conference on Robotics and Automation*, pp. 202-208.

[Krut(2005)] Krut, S., 2005, "A Force-Isotropic Underactuated Finger," *Proceedings of the 2005 IEEE International Conference on Robotics and Automation*, pp. 2325-2330, Barcelona, Spain.

[Laliberté and Gosselin(1998)] Laliberté, T., and Gosselin, C., 1998, "Simulation and Design of Underactuated Mechanical Hands," *Mechanism and Machine Theory*, 33, pp. 39-57.

[Laliberté and Gosselin(2003)] Laliberté, T., and Gosselin, C., 2003, "Actuation System for Highly Underactuated Gripping Mechanism," *US Patent No. 6 505 870*.

[Lobontiu(2002)] Lobontiu, N., 2002, "Compliant Mechanisms:

Design of Flexure Hinges," *CRC Press.*
[Lotti *et al.*(2005)] Lotti, F., Tiezzi, P., Vassura, G., Biagotti, L., Palli, G., and Melchiorri, C., 2005, "Development of UB Hand 3: Early Results," *Proceedings of the 2005 IEEE International Conference on Robotics and Automation*, pp. 4499-4504, Barcelona, Spain.
[Luo *et al.*(2004)] Luo, M., Mei, T., Wang, X., and Yu, Y., 2004, "Grasp Characteristics of an Underactuated Robot Hand," *Proceedings of the 2004 IEEE International Conference on Robotics and Automation*, pp. 2236-2241, New-Orleans, LA, USA.
[Massa and Gosselin(2003)] Massa, B.,and Gosselin, C., 2003, "Design and Development of an Underactuated Finger Based on Compliant Mechanisms," *Proceedings of 2003 CCToMM Symposium on Mechanisms, Machines, and Mechatronics*, pp. 58-72, St-Hubert, Canada.
[McCarthy(2000)] McCarthy, J. M., 2000, "Geometric Design of Linkages," *Springer-Verlag.*
[Smith(2000)] Smith, S. S., 2000, "Flexures: Elements of Elastic Mechanisms," *Gordon and Breach Science Publishers.*